Original Article

Dose accumulation in IMRT for left breast cancer determined by applying deformation registration

Ming Su[1,2], Guanzhong Gong[2], Xiaoping Qiu[1], Yong Yin[2]

[1]School of Nuclear Science and Technology, University of South China, Hengyang 421001, China; [2]Shandong Cancer Hospital and Institute, Shandong First Medical University and Shandong Academy of Medical Sciences, Jinan 250117, China

Contributions: (I) Conception and design: M Su, G Gong, Y Yin; (II) Administrative support: Y Yin; (III) Provision of study materials or patients: M Su, G Gong, Y Yin; (IV) Collection and assembly of data: M Su, X Qiu; (V) Data analysis and interpretation: All authors; (VI) Manuscript writing: All authors; (VII) Final approval of manuscript: All authors.

Correspondence to: Professor Yong Yin, PhD. Department of Radiation Oncology, Shandong Cancer Hospital and Institute, Shandong First Medical University and Shandong Academy of Medical Sciences, Jinan 250117, China. Email: yinyongsd@126.com.

Background: To evaluate the dosimetric changes in the target volume and organs at risk (OARs) of patients with left breast cancer (LBC) who underwent intensity-modulated radiation therapy (IMRT) based on a deformation registration (DF) method.

Methods: Sixteen patients with LBC treated with 6 MV X-ray IMRT were retrospectively analyzed. All targets included the lymph node drainage area and chest wall. All patients underwent CT for simulation of the primary positioning and repositioning. Primary and secondary treatment plans were developed using primary positioning CT (CT_1) and repositioning CT (CT_2) images to obtain $plan_1$ and $plan_2$, respectively. Rigid and DF of the dose distribution of $plan_2$ to CT_1 were applied; the results were then added to the dose distribution of $plan_1$, yielding $plan_{rig}$ and $plan_{def}$, respectively. The dosimetric differences between the target and OAR volumes of the four plans were compared.

Results: The clinical target volume of CT_2 was 8.74% less than that of CT_1. The planned target volume of CT_2 was 11.20% less than that of CT_1. The Dice similarity coefficients (DSCs) of the heart, left lung and right lung were significantly lower after than before DF (0.94±0.01 *vs.* 0.89±0.05, 0.96±0.01 *vs.* 0.91±0.03, and 0.96±0.01 *vs.* 0.92±0.03, respectively; t=3.83, 7.28, and 6.70, P<0.05, respectively). There were no significant differences in the dose-volume indices of the heart or left lung between $plan_1$ and the other plans, while the dose-volume indices were higher in $plan_{rig}$ than in $plan_{def}$.

Conclusions: Because of small changes in the target and OAR volumes during radiotherapy, we suggest the first IMRT plan could be used to evaluate the dose-volume indices of the lungs and heart for these patients.

Keywords: Breast cancer; dose addition; deformation registration (DF); dose assessment

Introduction

Intensity-modulated radiation therapy (IMRT) has gradually become an important part of comprehensive treatment for breast cancer (1). IMRT can improve the dose uniformity of a target and effectively reduce the dose and exposure volume of organs at risk (OARs), such as the heart and lungs (2). The current target range of breast radiotherapy includes the chest wall and breast cancer lymph node drainage area (3); these are complex targets for which target and OAR dose-volume assessments are essential. Radiation-induced heart injury (RIHI) and radiation-induced lung injury (RILI) are the two most problematic issues in the clinical treatment of left breast cancer (LBC) (4,5). Clinical studies have shown that

radiotherapy for LBC increases the probability of ischemic heart disease, pericarditis and valvular disease (6,7). Darby (8) found that the incidence of ischemic heart disease was proportional to the average radiation dose delivered to the heart and that the risk of morbidity began to increase within 20 years after radiotherapy. In the process of radiotherapy for breast cancer, respiration, target regression, heartbeat, weight loss and other factors change the shape and location of the target volume, resulting in decreased in the accuracy of the actual evaluation (9). Therefore, in theory, continued use of the initial plan to evaluate the target volume and dose delivered to OARs may lead to a large error between the planned dose and the actual radiation dose. In this study, breast cancer patients undergoing IMRT were selected, and the radiotherapy target volume included the supraclavicular lymph node drainage area and the chest wall. On this basis, the dose of two IMRT plans for breast cancer was acquired by rigid and deformation methods based on a deformation registration (DF) technique. The dose-volume indices of the target volume and normal tissues, such as the heart and lungs, were evaluated and compared with those of the original intensity modulation plan. The purpose of this study was to quantify the changes in the target and OAR dose-volume indices, including those in the chest wall and involved lymph nodes, in patients with breast cancer during IMRT.

Methods

General patient information

This study was a retrospective analysis of 16 female patients aged 27–66 years (median age of 42.5 years) with LBC who were treated from September 2016 to July 2018 at Shandong Cancer Hospital. The target volume included the lymph node drainage area plus the chest wall.

Image acquisition and design planning

The patients were placed in a supine position, after which the breast brackets were fixed, and their arms were lifted out to fully expose the left breast. A positioning scan was performed using a Philips large-aperture analog positioning machine. The scanning range extended from the ring membrane to the lung base to obtain the positioning CT image (CT_1). After CT_1 was introduced into a Varian Eclipse 13.5 system, the doctors outlined the whole breast clinical target volume, CTV_1, and performed CTV extrapolation to obtain the planned target volume, PTV_1, which delineated the OARs, including the heart and lungs. All delineations

were completed by the same physician. The IMRT plan was designed using the Varian Eclipse 13.5 system. The radiotherapy plan involved X-ray irradiation at 6 MV, and a radiotherapy dose of 50 Gy/25 fractions was planned as the total dose for CTV_1. A CT scan was performed following radiotherapy with 30–36 Gy/15–18 fractions using CT_1, and CT_2 was obtained. The physician sketched CTV_2, PTV_2 and the OAR volume according to CT_2. The two positioning methods and the target volume delineation standards were consistent. The reset plan dose was based on the initial planned dose of 50 Gy/25 fractions. Radiotherapy with 50 Gy/25 fractions for CTV_2 was used as $plan_2$.

DF and dose accumulation

CT_1 was set as the reference image, and CT_2 was set as the target image; CT_2 was separately processed for rigid and DF to CT_1 using Varian Velocity 3.2.1 software (shown in *Figure 1*). According to the registration image deformation point review and the vector field generated by the vector review, the rigid and deformation $plan_2$ dose was determined according to $plan_1$ and summed with the $plan_1$ dose to obtain $plan_{rig}$ and $plan_{def}$. The flow chart is shown in *Figure 2*.

Statistical analysis

Statistical analyses of the data included the following. (I) Changes in the target and OAR volumes: calculation of the CTV, PTV, and heart and lung volume change rates. (II) Target and OAR dose-volume indices: determination of the target volume D_2, D_{95}, D_{mean} and PTV exposure dose >95% volume (denoted as $V_{PTV95\%}$); the heart V_{20}, V_{30}, V_{40} and D_{mean}; the left lung V_5, V_{10}, V_{13}, V_{15}, V_{20} and V_{30}; and the right lung V_5, V_{10}, V_{13} and V_{15}. (III) Dice similarity coefficients (DSCs): calculation of the pre- and post-deformation CTV, PTV, and heart and lung DSC as DSC $=2|A \cap B|/(|A|+|B|)$, where A is CTV_1 and the OAR volume and B is CTV_2 and the OAR volume. (IV) Homogeneity index (HI): calculation of the target dose as HI $= (D_2 - D_{98})/D_{mean}$. (V) Conformity index (CI): calculation of the target dose CI as CI $= (V_{PTV95\%}/V_T) \times (V_{PTV95\%}/V_{PTV})$, where V_T is CTV and V_{PTV} is PTV. Statistical analysis was performed using SPSS 19.0 software. The data are presented as the mean ± standard deviation. A paired *t*-test was used to compare $plan_1$ and $plan_2$, $plan_1$ and $plan_{rig}$, $plan_1$ and $plan_{def}$, and $plan_{rig}$ and $plan_{def}$, with P<0.05 indicating a significant difference.

460

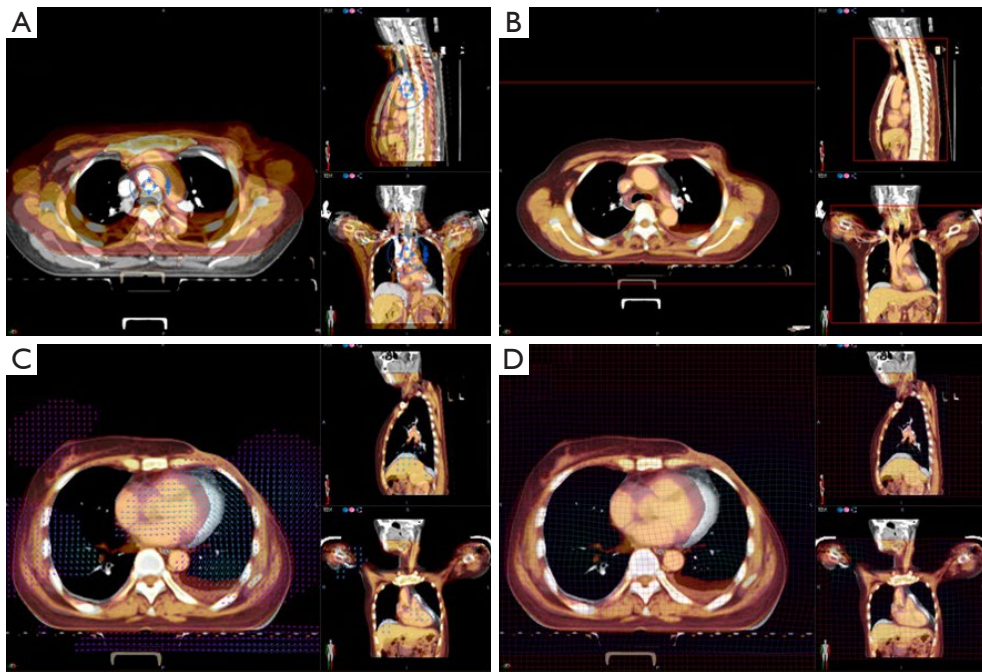Su et al. Dose accumulation in IMRT for LBC by DF

Figure 1 Deformation registration diagram. Before rigid registration (A); rigid registration (B); deformation registration vector audit (C); deformation registration grid audit (D).
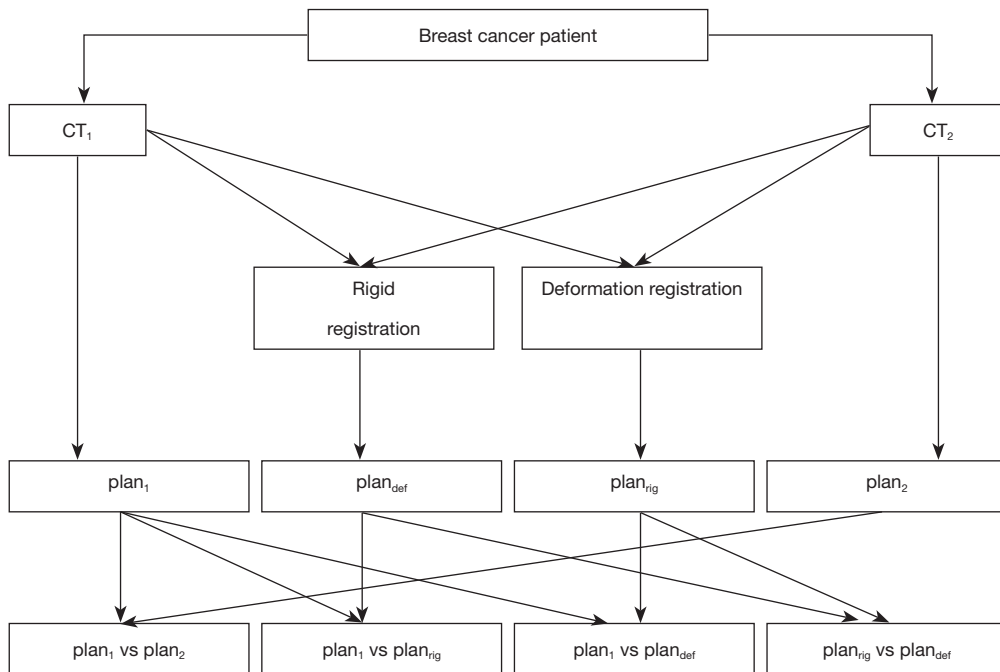

Figure 2 Schematic of the patient deformation registration process.

Table 1 Changes in target/OAR volumes ($\bar{x} \pm s$)

Organs	CT_1	CT_2	Rate (%)	t	P
PTV	928.6±222.7	799.4±189.6[a]	11.20± 6.5	6.793	0
CTV	697.4±204.0	641.6±204.1[a]	8.50±7.0	5.228	0
Heart	483.6±91.7	466.1±80.9[a]	3.10±7.0	2.113	0.052
Lung-L	1,178.1±226.9	1,173.6±237.7[a]	0.03±11.7	0.121	0.906
Lung-R	1,304.7±237.6	1,333.9±246.7[a]	−2.90± 12.9	−0.68	0.507

[a], compared with CT_1 group. OAR, organs at risk.

Table 2 Dose-volume indices of the heart for different plans ($\bar{x} \pm s$)

Group	V_{20}	V_{30}	V_{40}	D_{mean}	P
$Plan_1$	8.1±5.1	6.3±4.3	4.1±2.8	5.5±2.4	>0.05
$Plan_2$	8.1±4.8	5.3±3.7	3.3±2.7	5.0±2.2	>0.05
$Plan_{rig}$	8.2±4.9	6.2±4.1	3.9±2.7	5.7±2.3	>0.05
$Plan_{def}$	7.8±4.8	5.9±3.9	3.7±2.7	5.5±2.2	>0.05

There was no significant difference in dose volume index between $plan_1$ *vs.* $plan_2$, $plan_1$ *vs.* $plan_{rig}$, $plan_1$ *vs.* $plan_{def}$ and $plan_{rig}$ *vs.* $plan_{def}$.

Table 3 Dose-volume indices of the left lung for different plans ($\bar{x} \pm s$)

Group	V_5	V_{10}	V_{13}	V_{15}	V_{20}	V_{30}	P
$Plan_1$	55.7±5.1	42.5±3.9	38.1±4.2	35.7±4.4	30.7±4.4	24.8±4.3	>0.05
$Plan_2$	55.6±6.1	41.4±4.3	36.9±4.3	34.4±4.4	28.8±7.1	22.7±7.4	>0.05
$Plan_{rig}$	56.1±4.0	42.9±2.8	38.4±3.4	35.9±3.8	31.2±4.2	25.1±4.3	>0.05
$Plan_{def}$	56.0±4.2	42.4±3.1	37.8±3.7	35.3±4.0	30.6±4.3	24.4±4.3	>0.05

There was no significant difference in dose volume index between $plan_1$ *vs.* $plan_2$, $plan_1$ *vs.* $plan_{rig}$, $plan_1$ *vs.* $plan_{def}$ and $plan_{rig}$ *vs.* $plan_{def}$.

Results

Comparison of the target and OAR volumes between $plan_1$ and $plan_2$

Statistical analysis of CTV_1, CTV_2 and the OAR volume showed that PTV_2 and CTV_2 were significantly decreased by 11.2% and 8.5%, respectively (P<0.05). There were no significant differences in the lung volumes between the CT_2 and CT_1 groups (P>0.05). See *Table 1* for details.

Comparison of $plan_1$ and $plan_2$ dose volumes

For the V_{20}, V_{30}, V_{40} and D_{mean} of the heart, the $plan_2$ volumes were slightly less than the $plan_1$ volumes, but the

differences were not statistically significant (P>0.05). See *Table 2* for details. The V_5, V_{10}, V_{13}, V_{15}, V_{20} and V_{30} of the left lung were significantly lower in $plan_2$ than in $plan_1$ except for a slight increase in V_5; the difference was not statistically significant (P>0.05). See *Table 3* for details. In the right lung, the V_5, V_{10}, V_{13} and V_{15} in $plan_2$ were slightly lower than those in $plan_1$ except for a slight increase in V_5, and the differences were not statistically significant (P>0.05). See *Table 4* for details.

Comparison of $plan_1$ and $plan_{rig}$ dose-volume indices

The dose-volume indices based on rigid registration showed that the CI of the $plan_{rig}$ target volume changed

Table 4 Dose-volume indices of the right lung for different plans ($\bar{x} \pm s$)

Group	V_5	V_{10}	V_{13}	V_{15}	P
Plan$_1$	6.7±7.4	2.4±5.7	1.1±3.6	0.9±2.9	>0.05
Plan$_2$	7.7±8.5	2.8±6.3	1.3±4.0	0.9±2.0	>0.05
Plan$_{rig}$	7.5±7.6	2.2±5.8	1.2±3.8	0.9±2.9	>0.05
Plan$_{def}$	7.4±7.7	2.2±5.8	1.1±3.8	0.9±2.9	>0.05

There was no significant difference in dose volume index between plan$_1$ vs. plan$_2$, plan$_1$ vs. plan$_{rig}$, plan$_1$ vs. plan$_{def}$ and plan$_{rig}$ vs. plan$_{def}$.

Table 5 Comparison of the target CI and HI for different plans ($\bar{x} \pm s$)

Evaluation index	Plan$_1$	Plan$_2$	Plan$_{rig}$	Plan$_{def}$
CI	1.33±0.16	1.29±0.21[a]	1.08±0.12[b]	1.16±0.14[c,d]
HI	0.11±0.04	0.35±0.16[a]	0.38±0.13[b]	0.25±0.07[c,d]

[a], compared with plan$_1$ group, t=1.406, −6.421 , P<0.05; [b], compared with plan$_1$ group, t=6.943, −8.302, P<0.05; [c], compared with plan$_1$ group, t=−5.464, −9.481, P<0.05; [d], compared with plan$_{rig}$ group, t=−2.786, 3.053, P<0.05. HI, homogeneity index; CI, conformity index.

Table 6 DSCs pre- and post-deformation ($\bar{x} \pm s$)

Organs	Pre-deformation	Post-deformation	t	P
PTV	0.84±0.08	0.84±0.08[a]	1.025	0.322
CTV	0.86±0.11	0.85±0.11[a]	0.698	0.496
Heart	0.94±0.01	0.89±0.05[a]	3.833	0.002
Lung-L	0.96±0.01	0.91±0.03[a]	7.282	0
Lung-R	0.96±0.01	0.92±0.03[a]	6.701	0

[a], compared with the pre-deformation group.

from 1.08±0.12 to 1.33±0.16 with plan$_1$, and the difference was statistically significant (P<0.05). See *Table 5* for details. Compared with the plan$_1$ group, the plan$_{rig}$ group showed slight increase in the dose-volume indices of the heart and left and right lungs, but there were no significant differences between the groups (P>0.05). See *Tables 2-4* for details.

Comparison of plan$_1$ and plan$_{def}$ dose-volume indices

The dose-volume indices based on DF showed that the CI of the plan$_{def}$ target range changed from 1.16±0.14 to 1.33±0.16 with plan$_1$, and the difference was statistically significant (P<0.05). See *Table 5* for details. Compared with those in the plan$_1$ group, the dose-volume indices in the plan$_{def}$ group were essentially the same, and the differences were not statistically significant (P>0.05). See *Tables 2-4* for

details.

Comparison of plan$_{rig}$ and plan$_{def}$ dose-volume indices

Comparing the rigid registration plan with the DF plan showed that the plan$_{rig}$ target volume uniformity index of 0.38±0.13 decreased significantly to 0.25±0.07 for plan$_{def}$ (P<0.05, *Table 5*). The DSCs of the PTV, CTV, heart, left lung, and right lung in the plan$_{rig}$ and plan$_{def}$ groups were 0.84±0.08 and 0.84±0.08, 0.86±0.11 and 0.85±0.11, 0.94±0.01 and 0.89±0.05, 0.96±0.01 and 0.91±0.03, 0.96±0.01 and 0.92±0.03, respectively, and the differences were statistically significant (P<0.05, *Table 6*). For the OARs, the V_{20}, V_{30}, V_{40}, and D_{mean} of the heart were increased by 6.1%, 7.3%, 11.9%, and 4.3%, respectively, in the plan$_{rig}$ group compared with the plan$_{def}$ group; the V_5,

V_{10}, V_{13}, V_{15}, V_{20}, and V_{30} of the left lung were increased by 0.5%, 1.2%, 1.5%, 1.7%, and 2.7%, respectively; and the V_5, V_{10}, V_{13}, and V_{15} of the right lung were increased by 2.3%, 5.0%, 12.5%, and 6.7%, respectively. Paired t-tests of the abovementioned evaluation indices showed significant differences for the heart and left lung volumes (P<0.05) but not for the right lung (P>0.05). See *Tables 2-4* for details.

Discussion

IMRT for breast cancer can ensure that the target tumor volume receives the prescribed dose while reducing the dose delivered to normal tissues (10,11). In a study of 14 breast cancer patients treated with IMRT and planned dosimetry, Liu (12) found that IMRT plans can meet the clinical dosimetry demands of postoperative radiotherapy for LBC and have a better conformity. Clinical data show that the exposure volume (V_5–V_{30}) of the affected lung at different doses can better predict the incidence of radiation pneumonitis, and the average dose delivered to the heart with different exposure volumes (V_{20}, V_{30}, V_{40}, D_{mean}) can be compared (4,13,14). Because is helpful to predict the probability of RIHI, accurately calculating the dose delivered to OARs is crucial for predicting radiation damage in breast cancer patients. In the middle and late stages of breast cancer treatment, the location, shape and size of the target volume and surrounding normal tissues change to varying degrees, which may lead to an insufficient dose delivered to the target volume and an increased dose delivered to normal tissues, thus affecting the therapeutic efficacy. Therefore, accurate assessment of the dose-volume indices of lung and cardiac tissue is critical.

In this study, after 15 to 18 fractions of radiotherapy in breast cancer patients, a repeat CT scan was obtained, and the IMRT plan was revised. Then, the two planned doses were rigidly determined according to the deformation fields of their corresponding CT images by the DF technique. The deformation field was superimposed to obtain the $plan_{rig}$ and $plan_{def}$ groups. Comparison of the $plan_{rig}$ and $plan_1$ groups as well as the $plan_{def}$ and $plan_1$ groups showed that the changes in the CTV, PTV, heart and lung volumes were small, especially that in the CTV (<10%), and the deformation was matched. The dose-volume indices of all OARs were essentially consistent with those in the $plan_1$ group, with no significant differences. Varian Velocity, the DF software used in this study, is a clinically applicable deformable image registration (DIR) technique for image registration that utilizes a B-spline free-form deformation

algorithm. The B-spline algorithm is based on the Mattes formulation and consists of mutual information and proprietary methods not divulged by the vendor. The limited-memory Broyden-Fletcher-Goldfarb-Shanno optimization algorithm was used to find the optimal node value, with a maximum of 100 iterations and 20 corrections being used as a termination condition for the optimization algorithm (15). In an evaluation of velocity deformation accuracy, Palma *et al.* (16) suggested that the accuracy of DF ranges between 3 and 5 mm. Brock (17) showed that the average absolute error of DF is <2.5 mm. Schreibmann *et al.* (18) proved that B-spline deformation can simulate changes in lung volume within 3 mm. Hoffmann *et al.* (19) proved that velocity can reduce the average target registration error to a clinically acceptable level.

The DSCs of the heart and lungs post-deformation were significantly decreased compared with those pre-deformation (P<0.05). There were no significant differences in the dose-volume indices between the heart and lungs pre-deformation (P>0.05), and the dose-volume indices of the heart and left lung were significantly different post-deformation, which may have been caused by excessive deformation, leading to a superior CI in the $plan_{rig}$ and $plan_{def}$ groups. In this study, the DSCs of the organs post-deformation in this study were lower than those pre-deformation, indicating that the DIR was excessive in this study. Therefore, in this study, the post-deformation target and OAR dose-volume indices could not be used to evaluate the radiotherapy plan, and it was further confirmed that the initial plan could be used to evaluate the entire radiotherapy process.

In general, dose accumulation based on DF can be used to assess the target and OAR dose-volume indices throughout the course of radiation therapy. However, in patients with large changes in body position during treatment and large influences on the target volume, the contour difference between the two CT images was large. It is not appropriate to use the dose deformation and accumulation method to evaluate the target volume and dose variation in an OAR during radiotherapy (20). During radiotherapy in this study, shrinkage of the target volume was not obvious. The dose-volume indices of the OARs after DF were essentially consistent with those in the initial plan, and the organs remained at risk during the DF process. The excessive deformation caused the evaluation to be inaccurate. Therefore, the initial plan could be used to accurately predict the dose-volume indices of the heart and affected lung.

In summary, for patients with LBC, a synchronous radiotherapy target volume, including the lymph node

drainage area and the chest wall, and the dose-volume indices of the first planned OAR volume can be used for pretreatment evaluation due to less changes in the tumor and OAR morphology and volume. While prediction of the target and OAR volumes may be compromised during execution of the entire radiotherapy plan.

Acknowledgments

Footnote

Conflicts of Interest: All authors have completed the ICMJE uniform disclosure form (available at http://dx.doi.org/10.21037/tcr.2019.11.31). The authors have no conflicts of interest to declare.

Ethical Statement: The authors are accountable for all aspects of the work in ensuring that questions related to the accuracy or integrity of any part of this work are appropriately investigated and resolved. The study was conducted in accordance with the Declaration of Helsinki (as revised in 2013). This retrospective study was approved by the Institutional Ethics Review Board of the Shandong Cancer Hospital (No. 201809021). Medical record review was performed in accordance with Institutional Ethics Review Board guidelines. Informed consent was waived due to the retrospective nature of the study.

Open Access Statement: This is an Open Access article distributed in accordance with the Creative Commons Attribution-NonCommercial-NoDerivs 4.0 International License (CC BY-NC-ND 4.0), which permits the non-commercial replication and distribution of the article with the strict proviso that no changes or edits are made and the original work is properly cited (including links to both the formal publication through the relevant DOI and the license). See: https://creativecommons.org/licenses/by-nc-nd/4.0/.

References

1. Pignol JP, Truong P, Rakovitch E, et al. Ten years results of the Canadian breast intensity modulated radiation therapy (IMRT) randomized controlled trial. Radiother Oncol 2016;121:414.

2. Liu H, Chen X, He Z, et al. Evaluation of 3D-CRT, IMRT and VMAT radiotherapy plans for left breast cancer based on clinical dosimetric study. Comput Med Imaging Graph 2016;54:1-5.

3. Donovan EK, Corbett T, Vansantvoort J, et al. Radical chest wall resection and hyperfractionated accelerated radiotherapy for radiation-associated angiosarcoma of the breast: A safe and effective treatment strategy. Breast J 2018;24:245-52.

4. Aznar MC, Duane FK, Darby SC, et al. Exposure of the lungs in breast cancer radiotherapy: A systematic review of lung doses published 2010–2015. Radiother Oncol 2018;126:148-54.

5. Zhuang XF, Yang YM, Sun XL, et al. Late onset radiation-induced constrictive pericarditis and cardiomyopathy after radiotherapy: A case report. Medicine 2017;96:e5932.

6. Taylor CW, Kirby AM. Cardiac Side-effects From Breast Cancer Radiotherapy. Clin Oncol (R Coll Radiol)2015;27:621-9.

7. Nilsson G, Petra WN, Isacsson U, et al. Radiation dose distribution in coronary arteries in breast cancer radiotherapy. Acta Oncol 2016;55:959-63.

8. Darby SC, Ewertz M, McGale P, et al. Risk of ischemic heart disease in women after RT for breast cancer. N Engl J Med 2013;368:987-98.

9. Li Q, Tong Y, Yin Y, et al. Definition of the margin of major coronary artery bifurcations during radiotherapy with electrocardiograph-gated 4D-CT. Phys Med 2018;49:90-4.

10. Bazan JG, Dicostanzo DJ, Quick AM, et al. Radiation Dose to the Musculature of the Neck/Shoulder and Trunk in Women With Breast Cancer Undergoing Regional Nodal Irradiation: A Comparison of Intensity Modulated Radiation Therapy Versus 3D Conformal Radiation Therapy. Int J Radiat Oncol Biol Phys 2016;96:E57.

11. Pasquier D, Le Tinier F, Bennadji R, et al. Intensity-modulated radiation therapy with simultaneous integrated boost for locally advanced breast cancer: a prospective study on toxicity and quality of life. Sci Rep 2019;9:2759.

12. Schubert LK, Gondi V, Sengbusch E, et al. Dosimetric comparison of left-sided whole breast irradiation with 3DCRT, forward-planned IMRT, inverse-planned IMRT, helical tomotherapy, and topotherapy. Radiother Oncol 2011;100:241-6.

13. Wen G, Tan YT, Lan XW, et al. New Clinical Features and Dosimetric Predictor Identification for Symptomatic Radiation Pneumonitis after Tangential Irradiation in Breast Cancer Patients. J Cancer 2017;8:3795-802.

14. Hahn E, Jiang H, Ng A, et al. Late Cardiac Toxicity After

Mediastinal Radiation Therapy for Hodgkin Lymphoma: Contributions of Coronary Artery and Whole Heart Dose-Volume Variables to Risk Prediction. Int J Radiat Oncol Biol Phys 2017;98:1116.

15. Moriya S, Tachibana H, Kitamura N, et al. Dose warping performance in deformable image registration in lung. Phys Med 2017;37:16.

16. Palma DA, van Sörnsen de Koste JR, et al. A new approach to quantifying lung damage after stereotactic body radiation therapy. Acta Oncol 2011;50:509-17.

17. Brock KK. Results of a Multi-Institution Deformable Registration Accuracy Study (MIDRAS). Int J Radiat Oncol Biol Phys 2010;76:583-96.

18. Schreibmann E, Yang Y, Boyer A, et al. SU-FF-J-21: Image Interpolation in 4D CT Using a BSpline Deformable Registration Model. Med Phys 2005;32:1924.

19. Hoffmann C, Krause S, Stoiber EM, et al. Accuracy quantification of a deformable image registration tool applied in a clinical setting. J Appl Clin Med Phys 2014;15:4564.

20. Samavati N, Velec M, Brock KK. Effect of deformable registration uncertainty on lung SBRT dose accumulation. Med Phys 2016;43:233-40.